Journal of Sound and Vibration (2001) **241**(4), 653–679
doi:10.1006/jsvi.2000.3306, available online at http://www.idealibrary.com on IDEAL®

A GENERALIZED LOCAL LINEARIZATION PRINCIPLE FOR NON-LINEAR DYNAMICAL SYSTEMS

D. Roy and L. S. Ramachandra

Department of Civil Engineering, Indian Institute of Technology, Kharagpur 721 302, *India*
E-mail: *royd@civil.iitkgp.ernet.in*

(*Received* 15 *October* 1999, *and in final form* 28 *August* 2000)

Tangent spaces in non-linear dynamical systems are state dependent. Hence, it is generally not possible to exactly represent a non-linear dynamical system by a linear one over finite segments of the evolving trajectories in the phase space. It is known from the well-known theorem of Hartman and Grobman that a non-linear oscillator admits a linearization within a neighbourhood of any hyperbolic fixed point in the sense that the linearized flow bears a topological conjugacy to the non-linear flow within the same neighbourhood. This linearization is based on the construction of the tangent space to the non-linear vector field at the hyperbolic fixed point. Even though useful in bifurcation analysis, such a linearization procedure cannot be successfully applied to identically simulate the non-linear flow over the phase space because the functional form of the topological conjugacy is not known. With this in mind, an implicit approach to local linearization is evolved in this paper such that the tangent space of the linearized equation transversally intersects the tangent space to the non-linear dynamical system at that point in the state space where the solution vector is desired. Several numerical schemes for the implementation of this implicit and local linearization procedure are explored and illustrated with several numerical results. It is shown that the locally transversal linearization (LTL) procedure finally reduces the given set of non-linear ordinary differential equations (ODEs) to a set of transcendental algebraic equations with the desired solution vector as the unknown. The variables in the state space appear as unknown quantities in this approach. Finally, one arrives at non-linear Poincare maps for the non-linear oscillator. In this scheme, the characteristic time interval for the map is arbitrarily fixed. The methodology is found to be quite versatile for handling non-linear dynamical systems. In particular, it is verified that these schemes are capable of accurately predicting a wide spectrum of typically non-linear response characteristics, such as limit cycles, multi-periodicity, almost periodicity and chaos. For a limited class of response patterns, the principle proposed has another advantage in that the time step for integrating the non-linear ODEs need not be small. An improved and a more general higher order version of the LTL method is also considered. A distinct advantage of this higher version is in its improved ability for a closer simulation of phase-dependent time histories where a difference in the initial conditions leads to a phase difference in the realized solution history.

1. INTRODUCTION

In the literature, there exists a vast array of approximate analytical and numerical tools for analyses and direct integrations of non-linear dynamical systems. However, the diverse response patterns that a non-linear oscillator can potentially display is truly amazing and no known analytical technique is versatile enough to successfully predict all these complicated dynamical features. Among the available and popularly used analytical techniques, mention may be made of the classical Krylov–Bogoliubov averaging technique

0022-460X/01/140653 + 27 $35.00/0

[1], the secular perturbation theory [2, 3], the method of multiple scales [4, 5] an incremental harmonic balancing method [6], the homotopy method [7], a process analysis method [8], etc. These techniques are often observed to be too approximate for the prediction of quasi-periodic, limit-periodic and aperiodic (such as chaotic) orbits. Numerical integration methods, even though more versatile, are sometimes too sensitive to the choice of time-step size to be reliable (see references [9, 10]). A numeric-analytical phase-space linearization (PSL) method, proposed recently by Iyengar and Roy [11, 12] for the response analysis of a class of non-linear oscillators, has been found to correctly predict complicated dynamical trajectories arising out of a locally diverging or repelling nature of nearby trajectories. An advantage of this numeric-analytical scheme lies in the fact that it effectively combines the versatility of numerical schemes with the elegance and computational ease of analytical schemes. The essence of the PSL method is to replace a continuous non-linear vector field by a countable set of suitably constructed conditionally linear ones. Each of these conditionally linear fields is, in turn, valid over a short segment of the evolving trajectory projected on the phase space or equivalently on the time axis. It has further been pointed out that the procedure of such a local replacement of non-linear vector fields by linear ones is not unique. With suitable modifications, the explicit version of the PSL scheme has been applied to both deterministically and/or stochastically forced non-linear dynamical systems by Roy [13] and Iyengar and Roy [14]. It has been noted that this method has the subtlety to detect local instabilities in non-linear flows. Hence, it can correctly predict different types of non-linear phase flow patterns, including the quasi-periodic and chaotic ones, irrespective of their complexity.

The limited numerical success of the PSL method notwithstanding, a suitable theoretical foundation of the philosophy of the method is essential to correctly understand the precise relationship between the conditionally linear flow and the non-linear flow over a given time interval. Moreover, since the topological understanding of a non-linear flow around a given point on an evolving orbit is via the construction of a linear tangent space (see references [15, 16]), the linearized and non-linear flow patterns have to be related in terms of their respective tangent spaces. It is known that the tangent space of a system of non-linear ODEs is a function of the state variables themselves in contrast to the state-independent tangent spaces of a linear system. Thus, it is too ambitious to derive a time-invariant linear dynamical system whose evolution will, in general, precisely match that of a given non-linear system over any finite time interval. It may, however, be pertinent to ask if it is possible to construct a conditionally time-invariant and linear vector field over a given time interval such that the resulting flow is made to transversally intersect the non-linear flow at the right boundary of the time interval. The present paper may be considered to be an exploration of the possibilities for constructing such conditional and transversal linear systems. In particular, it is shown that considerations of transversality between tangent spaces of the linearized flow and the non-linear flow lead to a new implicit form of local linearization. This novel technique, referred to as the "locally transversal linearization" (LTL) method, strives to exactly satisfy the governing non-linear ordinary differential equations (ODEs) only pointwise at a countable number of unknown solution co-ordinates. In the present study, the entire solution class of non-linear oscillators has been broadly categorized into phase-dependent and phase-independent solutions. The more frequently observed phase-dependent solution, for instance, is the one where two distinct initial conditions lead to two topologically identical orbits (in the associated phase space), whose solutions histories are only separated by a phase difference. It is next argued that the LTL method is very accurately suited, irrespective of the chosen time step, towards obtaining solution points of non-linear oscillators in the phase-independent regime and not so much in the phase-dependent regime. However, a simple error analysis shows that even during

phase-dependent flows, one can put a bound on the absolute value of the error in terms of the chosen time step. In order to have an even more effective LTL-based scheme in the phase-dependent regime, a higher order LTL method is also proposed and this enables a more accurate pathwise (and not just pointwise) simulation of non-linear trajectories. Practical implementations of these methods are further illustrated with two workhorse dynamical systems in the literature, namely the Duffing and Lorenz oscillators. In particular, numerical implementations for the Lorenz system have been effected in a manner suitable for being adapted to any non-linear dynamical system irrespective of its dimensionality.

2. THE LTL METHODOLOGY

To begin with, consider a non-linear oscillator of the following state-space form:

$$\dot{x} = A(t)x + Q(x, t) + f(t) = V(x, t), \tag{1}$$

where $x \in R^n$, $A(t)$ is an $n \times n$ state-independent coefficient matrix associated with the linear terms, $f(t): T \subset R \to R^n$ is the external (non-parametric) force vector, $Q(x, t): T \times R^n \to R^n$ is that part of the vector field which is non-linear in x, and $V(x, t)$ stands for the entire vector field. Presently, it is assumed that the elements of $Q(x, t)$, $f(t)$ and $A(t)$ are C^k, $k \in Z^+$ continuous in x and t with $k \geqslant 1$. The initial condition vector to integrate equation (1) is denoted as $x_0 = x(t_0)$. Now let the time axis be ordered such that $t_0 < t_1 < t_2 < \cdots < t_i < \cdots$ and $h_i = t_i - t_{i-1}$, where $i \in Z^+$. The issue now is that of replacing the non-linear system of ODEs (1) by a suitably chosen set of n linear system of ODEs, wherein the ith linear system should, in a sense, 'closely' represent the non-linear flow over the ith time interval $T_i = (t_{i-1}, t_i]$. Let $\phi_t(.)$ and $\bar{\phi}_{t,i}(.)$, respectively, denote the vector solution flows of the non-linear system and the ith linearized system of ODEs. In the earlier studies by Roy [12] and Iyengar and Roy [13] for the development of the PSL method, the goal was set as to derive the ith linearized system of ODEs in such a way that $\bar{\phi}_{t,i}(.)$, approximates $\phi_t(.)$ as closely as possible uniformly over the semi-closed interval T_i. Unfortunately, the procedures to derive these linearized systems have been non-unique and validations in the form of numerical simulations have only been provided so far. A different and possibly more rigorous point of view is however adopted in the present study. Thus the objective, to begin with, is not to derive the linearized ODEs so as to remain everywhere 'close' to the non-linear flow, but to have the ODEs in such a manner that the given non-linear system is exactly satisfied at a countable number of points along the time axis or, equivalently, at a countable number of cross-sections, constructed transversal to the evolving flow. To use a more rigorous setting, let $\phi_t(x)$ be evolving on a compact manifold M, such that

$$\phi_t: M \times R \to M \tag{2}$$

is a C^k flow on M. Thus, for any choice of t, $\phi_t(x)$ is a C^k diffeomorphism $M \to M$ and the following simple relations hold:

$$\phi_{t_0} = \phi_0 = id_M, \qquad \phi_{t_{i-1}} \circ \phi_{h_i} = \phi_{t_i} \tag{3}$$

provided that the vector field is autonomous (note that an n-dimensional non-autonomous vector field can be posed as an $(n + 1)$-dimensional autonomous one). The set of all such C^k diffeomorphisms, $\phi_t(x)$, under the operation of composition 'o' form a group, G_ϕ. Now the

second of equations (3) may be interpreted in terms of two different group actions [16]. While the first is the R-action defined as

$$R \to G_\phi : t \to \phi_t \tag{4a}$$

the second is known as the Z-action:

$$Z \to G_\phi : j \to \phi_{t_j}. \tag{4b}$$

Here, Z denotes the set of all integers. Thus, the present objective may be stated as to derive a set of linear differential systems to obtain the same Z-action. At this stage, it should be apparent that these can at best be only conditionally linear, being conditioned upon their exactly satisfying the given non-linear differential system at a discrete number of time points, $S = \{t_i | i = 1, 2, 3, \dots\}$, but not necessarily elsewhere. This, in other words, implies that the conditionally linear flows have to transversally intersect the non-linear flow at least at the cross-sections sampled stroboscopically at every time point in S. For a one-dimensional dynamical system ($n = 1$), a pictorial representation of the scenario is as shown in Figure 1. More precisely, if the R-action of the derived ith linear flow is such that $\bar{\phi}_{t,i} : \bar{M}_i \times R \to \bar{M}_i$ is a diffeomorphism, then there will be an associated diffeomorphic Z-action, $\bar{f}_i$, relating the two successive cross-sections of intersections, $p_{i-1} = \{x_{i-1}, t_{i-1}\}$ and $p_i = \{x_i, t_i\}$. At this stage, it is worth noting that $\bar{f}_i$ may be interpreted as a smooth map from $\bar{M}_i$ to M, since p_{i-1} and p_i belong to both M and $\bar{M}_i$. Thus, from the weak transversality theorem (see reference [17]), it follows that such mappings which are transversal to M at a given section of intersection, p_i, form an open and everywhere dense set in the space of smooth maps $\bar{f}_i : M \to \bar{M}_i$. In other words, this implies that the procedures to derive the conditionally linear system of ODEs are non-unique and uncountably many. Here a convenient and easily adaptable methodology of linearization using LTL is first depicted.

For ease of implementation, it is presently decided to derive the locally linearized system such that it is also n-dimensional and is obtainable from the given non-linear system with simple and least alterations. Towards this, the linearized equation (with constant coefficients) is constructed by simply recasting the non-linear equation (1) over T_i as

$$\dot{\bar{x}} = A(t_i)\bar{x} + B(x_i, t_i)\bar{x} + f(t) = \bar{V}(\bar{x}, t), \tag{5a}$$

where

$$Q(x, t) = B(x, t)x \tag{5b}$$

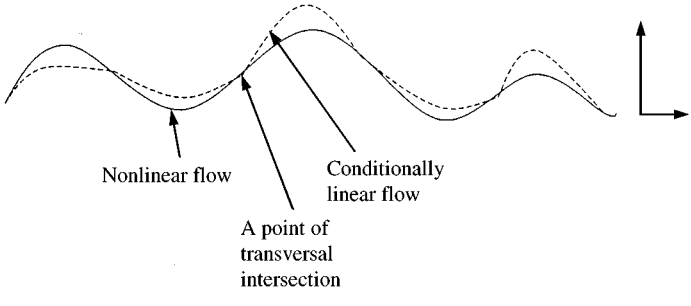

Figure 1. A schematic representation of the relationship between the non-linear and conditionally linearized flows.

provided that the vector function Q is separable with $B(x, t)$ finite in equation (5b). Equation (5a) is conditionally linear with constant coefficients given the precise value of the still unknown solution vector $x_i = x(t_i)$. Since equation (5a) is postulated to satisfy equation (1) at both the ends of the time segment T_i, the initial condition vector to equation (5a) is $x_{i-1} = x(t_{i-1})$. At this stage it will be useful to construct the locally linearized variational equation associated with equation (1) based on the point $x_i \in M$ as follows:

$$\dot{y} = D_{x=x_i} V(x, t) y = A(t) y + D_{x=x_i} Q(x, t) y, \tag{6}$$

where 'D' stands for the vector derivative or the Jacobian operator. It is observed that $D_{x_i} V(x, t)$ is the usual tangent map $T_{x_i} V$ based at the point $x_i \in M$ with the usual Riemann structure of inner product norms [15]. On the other hand, since equation (5a) is conditionally linear, the corresponding variational equation at x_i is obtainable by using the same vector field without the external forcing term, $f(t)$. Thus, the variational equation is

$$\dot{\bar{y}} = A(t_i)\bar{y} + B(x_i, t_i)\bar{y} = D_{x_i} \bar{V}(\bar{x}, t). \tag{7}$$

Here $D_{x_i} \bar{V}$ is the tangent space $T_{x_i} \bar{V}$ at $x_i \in M$. In fact, the unknown point, x_i, being a point of transversal intersection of the flows ϕ_i and $\bar{\phi}_i$, belongs to $M \cap \bar{M}$, a condition that can be viewed as a constraint on the constructed linearized flow. Consequently, a suitable constraint equation needs to be framed. Towards this, the solution of the linear system of equations (5a) is explicitly written down as

$$\bar{x}(t) = \psi(x_i, t, t_{i-1}) \left\{ x_{i-1} + \int_{t_{i-1}}^{i \leqslant t_i} \psi^{-1}(x_i, s, t_{i-1}) f(s)\, \mathrm{d}s \right\}, \tag{8}$$

where $\psi(x_i, t, t_{i-1})$ is the fundamental solution matrix. While the first term on the right-hand side of equation (8) represents the complementary solution, the second one stands for the particular integral due to the external forcing function, $f(t)$. Equation (8) may now be differentiated once to yield

$$\dot{\bar{x}}(t) = \dot{\psi}(x_i, t, t_{i-1}) x_{i-1} + \psi^{-1}(x_i, t, t_{i-1}) \dot{f}(t) + \dot{\psi}^{-1}(x_i, t, t_{i-1}) f(t). \tag{9}$$

The constraint condition, i.e., $x_i \in M \cap \bar{M}_i$, may be considered equivalent to the identify

$$\bar{x}(t_i) = x(t_i) = x_i. \tag{10}$$

In order to satisfy the above identity, $\bar{x}(t)$ and $\dot{\bar{x}}(t)$ from equations (9) and (10) are substituted into the non-linear equation (1) for $x(t)$ and $\dot{x}(t)$, respectively, at $t = t_i$. This leads to the following n algebraic and non-linear (transcendental) equations for the unknown vector x_i:

$$\mu(x_i, t_i, t_{i-1}) = 0, \tag{11a}$$

where the vector function μ is given by

$$\mu = \dot{\psi}(x_i, t_i, t_{i-1}) x_{i-1} + \psi^{-1}(x_i, t_i, t_{i-1}) \dot{f}(t_i) + \dot{\psi}^{-1}(x_i, t_i, t_{i-1}) f(t_i) - A(t_i)\bar{x}(t_i) - Q(x_i, t_i) - f(t_i). \tag{11b}$$

Attention is now focussed on the analytical expressions for the two tangent maps, $T_{x_i} V$ and $T_{x_i} \bar{V}$, given, respectively, by equations (6) and (7). It is clear that $T_{x_i} V$ is transversal to $T_{x_i} \bar{V}$

for almost all x_i except at a countable number of points satisfying the following n non-linear coupled algebraic equations:

$$D_x Q(x_i, t_i)x_i = B(x_i, t_i), \tag{12}$$

where only real roots, x_i, of the above equation are of interest. Consider, as a simple example, a one-dimensional ($n = 1$) case with $Q(x, t) = x^3$. In this case, equation (12) reduces to

$$2x_i^3 = 0. \tag{13}$$

In other words, $x_i = 0$ is the only point on the real line, R, where the original and reconstructed tangent spaces, $T_{x_i}V$ and $T_{x_i}\bar{V}$, fail to be transversal. Thus, if the solutions, x_i of equations (11) and (12) coincide, then the conditionally linear flow $\bar{\phi}_t$ does not transversally intersect the non-linear flow ϕ_t at p_i, thereby rendering the LTL method ineffective. An obvious way out is to translate t_i a little forward or backward such that x_i changes away from its singular value.

3. PHASE-DEPENDENT AND PHASE-INDEPENDENT SOLUTIONS

Non-linear response histories may be broadly classified based on their sensitivity to the chosen initial conditions. Taking, for instance, a couple of distinct initial conditions, the resulting time histories may be defined to be phase independent if they become asymptotically identical $t \to +\infty$. If more than one and a countably finite number of attracting limit sets exist, then the above definition still holds provided one restricts to the chosen initial conditions within the basin of attraction of only one of the limit sets. A phase-dependent solution, on the other hand, occurs in a manner so that any two such trajectories, originating from two different initial conditions, differ only by a constant or time-dependent phase along the time axis. The simplest example of a phase-independent solution is a sink, which is an asymptotically stable fixed point. In fact, for non-linear oscillators externally forced by a periodic excitation, the one-periodic solution is mostly phase independent. Multi-periodic, quasi-periodic and chaotic solutions are, on the other hand, phase dependent. If the oscillator passes into the phase-dependent regime, then for a given set of $p \in Z^+$ different initial conditions, a bundle of p distinct solutions will exist. Now consider the projections $\Sigma_i : M \times R \to M | t = t_i$, $i = 0, 1, 2, 3 \ldots$. If $\Sigma_0 \subset M$ consists of a countable infinity of initial conditions, i.e., $\Sigma_0 = \{x_0^{(k)} | k = 1, 2, \ldots, \infty\}$, then $\Sigma_i \subset M$, will also consist of a countable infinity of distinct points, $\{x_i^{(k)} | k = 1, 2, 3, \ldots, \infty\}$. In reality, the maps $f^i = \Sigma_0 + \Sigma_i$ are diffeomorphic for every i and for a sufficiently small $h_i = t_i - t_{i-1}$, since x_0^k has to get transformed to $x_i^{(k)}$ for any k. The diffeomorphisms, f^i, may readily be generated from a repeated application of the LTL procedure using equations (8) and (11a). It may now be noted that equation (11a) which is supposed to search for the correct solution, $x_i^{(k)}$ at $t = t_i$, has the initial condition $x_{i-1}^{(k)}$ as a parameter. However, due to a lack of a sufficiently accurate path information in the LTL procedure described so far, the conditionally linear equation (5a), based at the initial condition $x_{i-1}^{(k)}$, attempts to transversally intersect the nearest available non-linear trajectory at $t = t_i$ among the possible bundle of trajectories. In other words, given the initial condition, $x_{i-1}^{(k)}$, and more than one possible solutions $\{x_i^{(l)} | l = 1, 2, 3 \ldots\}$ at $t = t_i$, the solution vector, which is actually found, is not necessarily the desired one, i.e., x_i^k. In fact, the found solution $x_i^{(l)}$ in the solution set $\{x_i^{(l)} | l = 1, 2, 3 \ldots\}$ is closest, in the Euclidean sense, to the initial guess that the user provides for the solution vector. A graphical representation of the scenario for the simplest one-dimensional case ($n = 1$) is provided in Figure 2(a). Here solid lines indicate

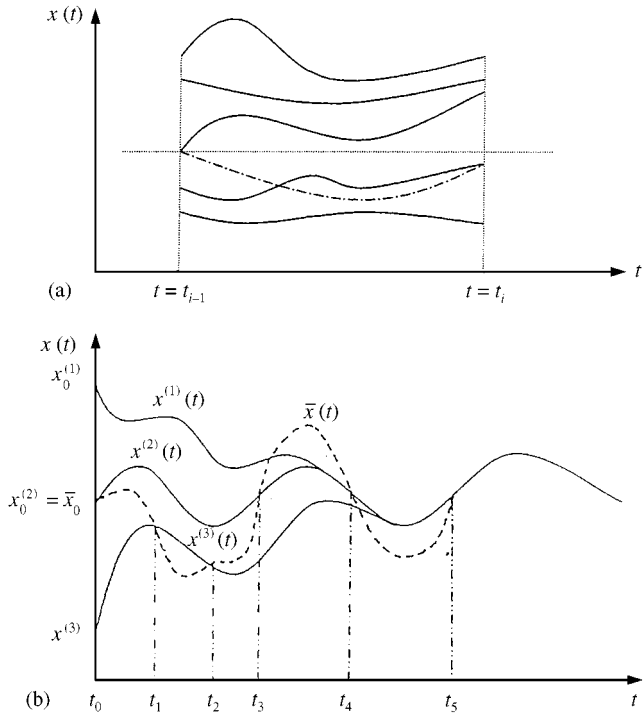

Figure 2. (a) A possible source of error in the LTL method during the transient regime: ——, exact; –·–·–·–, LTL; (b) unique intersections in the phase-independent regime.

five of the evolving non-linear trajectories over the time segment h_i. The dashed line, on the other hand, is the conditionally linear trajectory based at the initial condition $x_{i-1}^{(3)}$. Let the initial guess for x_i be $x_{i-1}^{(3)}$ itself. Then, as is clear from the figure, the closest zero of the transcendental function μ in equation (11a) is $x_i^{(2)}$ and not $x_i^{(3)}$, which is the desired one. It is also apparent from this figure that a higher accuracy for phase-dependent trajectories in the LTL method should demand a smaller time-step size. It is, however, important to note that in the phase-independent regime, the LTL method yields an exact mapping relating x_{i-1} to x_i irrespective of the chosen time step as the steady state is approached. A simple one-dimensional illustration is provided in Figure 2(b), wherein time histories of three phase-independent trajectories (solid lines), $x^{(1)}(t)$, $x^{(2)}(t)$ and $x^{(3)}(t)$ evolving, respectively, with initial conditions $x_0^{(1)}$, $x_0^{(2)}$ and $x_0^{(3)}$, are shown schematically. In the same figure, the dotted line, denoted by $\bar{x}(t)$, represent the LTL solution whose initial condition is set as $\bar{x}_0 = x_0^{(2)}$. Since in the steady state (say, for $t \geqslant t_5$), one virtually has the equality $x^{(1)}(t) = x^{(2)}(t) = x^{(3)}(t)$, the LTL-based solution $\bar{x}(t)$ should have unique intersection points with the original flow *irrespective of the chosen time-step size.*

4. ERROR ESTIMATES

While the LTL method, developed thus far, fails to make proper use of the available information on initial conditions in the transient regime, it is of interest to have an estimate of the error order for a better understanding of the procedure. In contrast, the LTL method yields an exact mapping relating x_{i-1} to x_i during phase independence. The importance of

an error estimate in this case, however, is to have an understanding of the extent to which the linearized flow, as constructed via LTL, falls away from the non-linear flow in between the co-ordinates x_{i-1} and x_i. Let the vector-valued signed error be defined as

$$E(t) = x(t) - \bar{x}(t). \tag{14}$$

Now towards estimating the error measure, a system of ODEs for $E(t)$ may be readily obtained by subtracting equation (5a) from equation (1):

$$\dot{E} = A(t)E + B(x, t)x - B(x_i, t_i)\bar{x}. \tag{15}$$

The above equation is valid only over the interval T_i. To keep track of the initial condition, say x_0^j, it is convenient to replace x_i in equation (15) by x_i^j. By adding and substituting $B(x_i^j, t_i)$, equation (15) may be recast as

$$\dot{E} = [A(t) + B(x_i^j, t_i)]E + [B(x, t) - B(x_i^j, t_i)]x. \tag{16}$$

It is now assumed that the 1-jet, $j_x^1 = \{x(t), D_t(x(t))h\}$ [15] of the process $x(t)$ exists and is bounded for all realizable vector values of $x(t)$. For notational convenience, $D_t(x)$ is denoted as $\dot{x}(t)$ in what follows.

Phase-dependent regime: Given x_i^j to be the solution obtained via LTL, the initial condition will be x_{i-1}^k where $k \neq j$. Thus, for $t_{i-1} < t \leqslant t_i$, one has, via a forward Taylor expansion about x_{i-1}^k,

$$x(t) - x_i^j = (x_{i-1}^k - x_i^j) - \dot{x}_{i-1}^k(t - t_{i-1}) + O(t - t_{i-1})^2. \tag{17}$$

It is important to note here that the above expansion constitutes a germ [15] to the original trajectory through x_{i-1}^k, which is different form the trajectory through x_i^j. Substituting equation (17) into equation (15) followed by integration leads to

$$E(t) = c(t) + \int_{t_{i-1}}^{t} u(s)E(s)\,\mathrm{d}s. \tag{18}$$

The vector-values functions $c(t)$ and $u(t)$ have the following form:

$$c(t) = E(t_{i-1}) + A_1(t - t_{i-1}) + A_2(t - t_{i-1})^2 + O(t - t_{i-1})^3, \tag{19a}$$

$$u(t) = A(t) + B(x_i^j, t_i), \qquad A_1 = E(t - t_{i-1}) + b_m x_{i-1}^k(x_{i-1}^k - x_i^j), \tag{19b, c}$$

$$A_2 = (b_m/2)\{(x_{i-1}^k)^2 + 2x_{i-1}^k\dot{x}_{i-1}^k - x_i^j x_{i-1}^k\}(t - t_{i-1})^2. \tag{19d}$$

In the above expressions, b_m stands for a finite upper bounds to the bounded function $B(x, t)$. Equation (18) is now recast as the following inequality by taking modulii (square root of the inner product) of various terms appropriately:

$$|E(t)| \leqslant |c(t)| + \int_{t_{i-1}}^{t} |u(s)|\,|E(s)|\,\mathrm{d}s. \tag{20}$$

The above inequation is now in a form for the application of Bellman–Grownwall lemma (see reference [18]):

$$|E(t)| \leqslant |c(t_{i-1})| \exp\left(\int_{t_{i-1}}^{t} |u(s)|\,\mathrm{d}s\right) + \int_{t_{i-1}}^{t} \dot{c}(s)\,\mathrm{sgn}(c(s))\left(\exp\int_{s}^{t} |u(\tau)\,\mathrm{d}\tau\right)\mathrm{d}s, \tag{21}$$

where, in the above expression, sgn(.) stands for the usual signum function. Since $\dot{c}(s) \approx O(1)$, exponential of a bounded function is also of $O(1)$ and $c(t_{i-1})$ is $O(t - t_{i-1})$, the right-hand side of the above inequation is $O(t - t_{i-1})$. Thus in the transient regime

$$|E(t)| \leqslant O(t - t_{i-1}). \tag{22}$$

Phase-independent regime: In contrast to the transient case, in the steady state the jet $j^n_{x(t)}$ of $x(t)$ based on x^k_{i-1} tends to pass through x^k_i as n is made indefinitely large. As noted earlier, this is because of the uniqueness of the non-linear flow irrespective of the chosen initial conditions. In other words, it means that

$$\lim_{n \to \infty} j^n_{x(t)=x^k_{i-1}} = \lim_{n \to \infty} j^n_{x(t)=x^k_i}. \tag{23}$$

Thus, for $t_{i-1} < t \leqslant t_i$, the original trajectory, $x(t)$, may be obtained by a back Ward Taylor expansion based on the co-ordinate x^k_i as follows:

$$x(t) - x^k_i = \dot{x}^k_i(t - t_i) + O(t - t_i)^2. \tag{24}$$

In this case, again, the error equation may be put in a form similar to equation (18) as

$$E(t) = c_s(t) + \int_{t_i}^{t} u(s)E(s)\,\mathrm{d}s. \tag{25}$$

Here the integration on the right-hand side has to be performed backwards in time. The expression for $c_s(t)$ is

$$c_s(t) = E(t_{i-1}) + B_1(t - t_i)^2 + O(t - t_i)^3, \tag{26}$$

$$B_1 = 0{\cdot}5 b_m x^k_i \dot{x}^k_i. \tag{27}$$

The expression for $u(s)$ remains the same as in equation (19b). The following inequality is thus arrived at:

$$|E(t)| \leqslant |c_s(t)| + \int_{t_i}^{t} |u(s)|\,|E(s)|\,\mathrm{d}s \tag{28}$$

Now a straightforward application of the Bellman–Gronwall lemma, as in the previous case, finally leads to

$$|E(t)| \leqslant O(t - t_i)^2. \tag{29}$$

5. HIGHER ORDER LTL PROCEDURES

Given the importance and frequent occurrences of the phase-independent and transient solutions in non-linear dynamical system, it is important to derive other forms of LTL schemes with capabilities to remain close to the original path from a given initial condition as followed by the non-linear system itself, provided that the chosen time step is sufficiently small. In what follows, a method for deriving consistently higher order and path-sensitive LTL-based ODEs is outlined. Towards this, the set of n conditionally linearized equations (5a) is augmented to twice its dimension and written as

$$\ddot{\dot{x}} = [A(t_i) + B(x_i, t_i)]\dot{\dot{x}} + \dot{f}(t). \tag{30}$$

It is easy to see that the above system has an additional central eigenspace. The non-uniqueness of solutions in central eigenspaces may be effectively exploited to introduce the desired path sensitivity. However, instead of solving the linearized system in this form, equation (30) is projected in the following form:

$$\ddot{\bar{x}} = [K(x_i, t_i)]\bar{x} + q(t), \tag{31}$$

where

$$[K(x_i, t_i)] = [A(t_i) + B(x_i, t_i)]^{\mathrm{T}}[A(t_i) + B(x_i. t_i)], \tag{32a}$$

$$q(t) = [A(t_i) + B(x_i, t_i)]f(t) + \dot{f}(t), \tag{32b}$$

Solution of the system of equations (31) may be constructed in the same way as in equation (8) provided it is written in the form of $2n$ first order equations as

$$\dot{X}(t) = G(x_i, t_i)X(t) + g(t), \tag{33}$$

where

$$[G(x_i, t_i)] = \begin{bmatrix} 0 & I_{n\times n} \\ K(x_i, t_i) & 0 \end{bmatrix}, \qquad g(t) = \begin{Bmatrix} 0 \\ q(t) \end{Bmatrix}. \tag{34}$$

Over the semi-closed interval T_i, the initial conditions for integrating equation (33) will be $(x_{i-1}\ \dot{x}_{i-1} = V(x_{i-1}, t_{i-1})\}$. In equations (34), $I_{n\times n}$ stands for an $n \times n$ identity matrix and 0, for a zero matrix of the same order. One therefore observes that the augmented LTL system (33), henceforth referred to as the first level LTL system, starts from the section Σ_{i-1} with the correct slope of the original state variables, $x(t)$. Thus, the conditionally linearized state variables, $\bar{x}(t)$, corresponding to the system in equation (5a) which is henceforth called the zeroth-level LTL system, obviously simulate the non-linear flow better. In precisely the same way as for the derivation of the first-level LTL system, even higher levels of LTL systems may be consistently derived for higher and higher accuracy in the phase-dependent and/or transient regimes. For example, if one constructs the second-level LTL system, consisting of $3n$ conditionally linearized first order ODEs, then the initial conditions to this system, valid over T_i will be $\{x_{i-1}, \dot{x}_{i-1}, \ddot{x}_{i-1}\}$, where

$$\ddot{x}_{i-1} = D_{x=x_{i-1}}\{V(x, t)\}\dot{x}_{i-1}. \tag{35}$$

In the above identity, $D_{x=x_{i-1}}(V)$ stands for the Jacobian operator on the non-linear vector field computed at $x = x_{i-1}$.

An error analysis similar to that presented in section 4 may be repeated for different higher levels of LTL systems with no change in the definition of the error function as in equation (14). Considering, for instance, the first-level LTL approach, the non-linear dynamical system (1) is once differentiated to yield

$$\ddot{x} = [\dot{A}(t) + A^{\mathrm{T}}(t)A(t)]x + [A(t)B(x, t) + A(t)D_xQ(x, t) + D_xQ(x, t)B(x, t)]x$$
$$+ [A(t) + D_xQ(x, t)]f(t) + \dot{f}(t). \tag{36}$$

Now defining an augmented error vector function $\hat{E}(t) = \{E(t)\ \dot{E}(t)\}^{\mathrm{T}} \in R^{2n}$, one may readily derive a set of $2n$ first order equations for $\hat{E}$. A local estimate of $\hat{E}(t)$ over the interval T_i using Grownwall's lemma (as in section 4) again leads to $\hat{E}(t) \leqslant O(h_i)$. This immediately implies that the desired error vector $E(t) \leqslant O(h_i^2)$ in the phase-dependent or transient

regime. Consequently, for an n-level LTL system, one may readily show that $E(t) \leqslant O(h_i^{n+1})$ locally in the phase-dependent regime. Of course, it needs to be noted here that this improved accuracy is obtainable only with a considerably higher computational cost.

6. ILLUSTRATIVE EXAMPLES

The LTL principles outlined so far will now be illustrated with a few examples of well-known non-linear systems, widely referred in the literature. The first example is that of the single-degree-of-freedom (s.d.o.f.) hardening Duffing (HD) oscillator, representing the single-modal bending vibrations of a beam with geometric non-linearity (see, for example, the monograph by Yu [19]) and governed by the following second order non-linear ODE:

$$\ddot{x} + 2\pi\varepsilon_1\dot{x} + 4\pi^2\varepsilon_2(1 + x^2)x = 4\pi^2\varepsilon_3\cos(2\pi t). \tag{37}$$

For s.d.o.f. oscillators, it is more convenient to apply the LTL procedure to the second order ODEs directly instead of reducing them to a couple of first order ODEs. Thus, for the HD oscillator, the conditionally linearized equation over the interval T_i and with initial conditions $\{x_{i-1}, \dot{x}_{i-1}\}$ is written down as

$$\ddot{x} + 2\pi\varepsilon_1\dot{x} + 4\pi^2\varepsilon_2\beta_1 x = 4\pi^2\varepsilon_3\cos(2\pi t) \qquad \beta_i = 1 + x_i^2. \tag{38a, b}$$

The two eigenvalues associated with the auxiliary part of equation (38a) are

$$\lambda_{1,2}^{(i)} = \pi\{-\varepsilon_1 \pm \sqrt{(\varepsilon_1^2 - 4\varepsilon_2\beta_i)}\}. \tag{39}$$

Depending on the value of the argument within the square root, the eigenvalues may be either be real or complex conjugates. For all practical purposes, however, one has $0 < \varepsilon_1 \ll 1$, $\varepsilon_2 > \varepsilon_1$, $\beta_i \geqslant 1$, thereby ensuring that $4\varepsilon_2\beta_i > \varepsilon_1^2$. This in turn implies that the eigenvalues are complex conjugates and are

$$\lambda_{1,2}^{(i)} = -\pi\varepsilon_i \pm \mathrm{j}\alpha_i(\beta_i), \qquad \alpha_i(\beta_i) = \pi\sqrt{4\varepsilon_2\beta_i - \varepsilon_1^2}. \tag{40}$$

It is noted that in the above equation $\mathrm{j} = \sqrt{-1}$. The complete solution of the conditionally linear equation (38a) may now be written as

$$\bar{x}(t) = \exp(-\pi\varepsilon_1(t - t_{i-1}))(C_1^{(i)}\cos(\alpha_i t) + C_2^{(i)}\sin(\alpha_i t)) + p_i(t), \tag{41a}$$

$$C_1^{(i)} = (E_2D_1 - E_1D_2)/(E_2F_1 - E_1F_2), \quad C_2^{(i)} = (F_2D_1 - F_1D_2)/(F_2E_1 - F_1E_2), \tag{41b, c}$$

$$F_1 = \cos(\alpha_i t_{i-1}), \qquad F_2 = -\pi\varepsilon_1\cos(\alpha_i t_{i-1}) - \alpha_i\sin(\alpha_i t_{i-1}), \tag{41d, e}$$

$$D_1 = \bar{x}_{i-1} - p_i(t_{i-1}), \qquad D_2 = \dot{\bar{x}}_{i-1} - \dot{p}_i(t_{i-1}), \tag{41f, g}$$

$$E_1 = \sin(\alpha_i t_{i-1}), \qquad E_2 = -\pi\varepsilon_1\sin(\alpha_i t_{i-1}) + \alpha_i\cos(\alpha_i t_{i-1}). \tag{41h, i}$$

In equation (41a), $p_i(t)$ denotes the conditionally particular solution and the rest of the terms on the right-hand side denote the conditionally complementary solution of the linearized equation. The particular part of the solution is given by

$$p_i(t) = \frac{\varepsilon_3(\varepsilon_2\beta_i - 1)\cos(2\pi t) + \varepsilon_1\varepsilon_3\sin(2\pi t)}{(\varepsilon_2\beta_i - 1)^2 + \varepsilon_1^2} = A_p\cos(2\pi t) + B_p\sin(2\pi t). \tag{42}$$

Now, deriving the expression for $\bar{x}(t)$, it is simple to find out analytical expressions for $\dot{\bar{x}}(t)$ and $\ddot{\bar{x}}(t)$ in terms of the unknown parameter β_i. Substitution of these expressions in the original non-linear equation (37) for the HD oscillator at $t = t_i$ finally results in a transcendental algebraic equation in β_i and hence x_i. This completes the exercise of deriving the zeroth order LTL system for the HD oscillator.

For a more general implementation of the LTL procedures for higher-dimensional dynamical systems, attention is now turned on the second example which is extensively studied, three dimensional and autonomous Lorenz system (see reference [20] and the important monograph by Sparrow [21]). The non-linear equations are

$$\dot{x}_1 = A(x_2 - x_1), \qquad \dot{x}_2 = x_1(R - x_3) - x_2, \qquad \dot{z} = x_1 x_2 - B x_3. \tag{43}$$

The Lorenz system is probably the simplest example of a non-linear hydrodynamic system describing Rayleigh–Benard convection and is the first known system to be chaotic. Defining the three-dimensional state vector $X = (x_1 \;\; x_2 \;\; x_3)^{\mathrm{T}}$, the corresponding linearized vector $\bar{X} = (\bar{x}_1 \;\; \bar{x}_2 \;\; \bar{x}_3)^{\mathrm{T}}$ and restricting attention, as before, on the semi-closed (time) interval T_i, a zeroth-level LTL system (non-unique) may be constructed as

$$\dot{\bar{X}} = [C(X_i)]\bar{X}, \tag{44}$$

where the conditionally constant 3×3 coefficient matrix $C(X_i)$ may be formed as

$$[C(X_i)] = \begin{bmatrix} -A & A & 0 \\ R & -1 & -x_{1,i} \\ x_{2,i} & 0 & -B \end{bmatrix}. \tag{45}$$

The conditional solution of the linearized system at $t = t_i$ is

$$\bar{X}(t_i) = [M][D][M]^{-1} X_{i-1}. \tag{46}$$

In equation (46), $[D] = \mathrm{diag}[\exp\{h_i \;\; \lambda_{1,i} \;\; \lambda_{2,i} \;\; \lambda_{3,i})\}]$ is the 3×3 diagonal matrix depending on the conditional eigenvalues, which may be found directly from the cubic characteristic equation

$$\lambda_{j,i}^3 + a\lambda_{j,i}^2 + b\lambda_{j,1} + c = 0, \quad j = 1, 2, 3, \tag{47}$$

where

$$a = 1 + A + B, \qquad b = A(1 + B - R) + B, \qquad c = A[B(1 - R) + x_{1,i}x_{2,i}]. \tag{48}$$

The three roots of equation (46) are available in the closed form [22]. Towards this, the following transformation is first effected:

$$\lambda_{j,i} = \bar{\lambda}_{j,i} - b/3. \tag{49}$$

This results in

$$\bar{\lambda}_{j,i}^3 + p\bar{\lambda}_{j,i} + q = 0. \tag{50}$$

Letting $r = (p/3)^3 + (q/2)^2$, the three roots, for the case when only one of them is real, are

$$\bar{\lambda}_{1,i} = u + v, \quad \bar{\lambda}_{2,i} = -0{\cdot}5(u+v) + (\sqrt{3}/2)(u-v)\mathrm{j}, \quad \bar{\lambda}_{3,i} = -0{\cdot}5(u+v) - (\sqrt{3}/2)(u-v)\mathrm{j}, \tag{51a}$$

$$u = \sqrt[3]{-0{\cdot}5q + \sqrt{r}}, \qquad v = \sqrt[3]{-0{\cdot}5q - \sqrt{r}}. \tag{51b}$$

It is known that the above roots will be all real for $r \leqslant 0$ and one real (positive) with the other two complex conjugates for $r > 0$. It may be noted here that conditional matrix of eigenvectors, $[M]$, in equation (46) are functions of the vector $\bar{X}_i = X_i$ and may be explicitly constructed only when the initial guess for this unknown vector is provided. Now, differentiation of equation (46) once at $t = t_i$ yields

$$\dot{\bar{X}}_i = [M][\dot{D}]_{t=t_i}[M]^{-1}X_{i-1}, \tag{52}$$

since $\bar{X}_{i-1} = X_{i-1}$. Thus, the desired non-linear algebraic equations in X_i are readily derived by substituting equation (52) in the given non-linear system of ODEs (43) at $t = t_i$. These three algebraic equations may be written in a vector form as

$$[M(X_i)][\dot{D}(X_i)]_{t=t_i}[M(X_i)]^{-1} - [C(X_i)]X_i = 0. \tag{53}$$

It may be noted that the process of deriving the conditional eigenvalues $\lambda_i(X_i)$ and the associated matrix $[M(X_i)]$ of conditional eigenvectors is rather involved, especially for a large m.d.o.f. dynamical system and the required non-linear vector function (as in the LHS of equation (53)) may only be formed implicitly in terms of the unknown solution X_i starting with a guess value. In the present study, a globally convergent non-linear equation solver based on line searches and backtracking along the Newton directions (see reference [7]) has been adopted for finding the desired roots at successive time instants.

Simpler forms of the zeroth-level LTL systems may be developed for the Lorenz system in case certain constraints on the response are imposed. One such conditionally uncoupled and the simplest possible zeroth-level LTL system is given by

$$\dot{\bar{x}}_1 = \beta_1\bar{x}_1, \qquad \dot{\bar{x}}_2 = \beta_2\bar{x}_2, \quad \dot{\bar{x}}_3 = \beta_3\bar{x}_3. \tag{54}$$

The local solutions of the above set of ODEs are

$$\bar{x}_{j,i} = x_{j,i-1}\exp(\beta_1(t - t_{i-1})), \quad j = 1, 2, 3. \tag{55}$$

Clearly, using this form of LTL and given a three-dimensional initial condition vector $\{x_{j,0} | j = 1, 2, 3\}$, the constraint on the locally linearized flows is that any element in resulting solution vectors $\{\bar{x}_{j,i} | j = 1, 2, 3; i = 1, 2, \dots\}$ cannot change its sign (from positive to negative and *vice versa*) from that of the corresponding element in the initial condition vector. While this is a serious restriction for a typical chaotic orbit of the Lorenz system, a large class of limit sets including fixed points for the Lorenz system should be readily detectable using the LTL system (54). Finally, three non-linear algebraic equations in terms of the three unknown coefficients, $\beta_1, \beta_2, \beta_3$, valid over T_i may be readily found by substituting the linear solutions (55) in the non-linear ODEs (43). These non-linear equations are

$$\beta_1 x_{1,i-1}\exp(\beta_1 h_i) - A(x_{2,i-1}\exp(\beta_2 h_i) - x_{1,i-1}\exp(\beta_1 h_i)) = 0, \tag{56a}$$

$$\beta_2 x_{2,i-1}\exp(\beta_2 h_i) - x_{1,i-1}\exp(\beta_1 h_i)(R - x_{3,i-1}\exp(\beta_3 h_i)) + x_{2,i-1}\exp(\beta_2 h_i), \tag{56b}$$

$$\beta_3 x_{3,i-1}\exp(\beta_3 h_i) - x_{1,i-1}\exp(\beta_1 h_i)x_{2,i-1}\exp(\beta_2 h_i) + Bx_{3,i-1}\exp(\beta_3 h_i). \tag{56c}$$

To start with, a good initial guess vector for $\{\beta_1\ \beta_2\ \beta_3\}^{\mathrm{T}}$ will be $\{0\ 0\ 0\}^{\mathrm{T}}$.

Example of the simplest first-level LTL system: The simplest possible first-level LTL system for the Lorenz oscillator may be constructed as a set of three conditionally uncoupled second order linear ODEs, given by

$$\ddot{\bar{x}}_1 - \beta_1^2 \bar{x}_1 = 0, \qquad \ddot{\bar{x}}_2 - \beta_2^2 \bar{x}_2 = 0, \qquad \ddot{\bar{x}}_3 - \beta_3^2 \bar{x}_3 = 0. \tag{57}$$

The above form for the vector field has been so chosen that the eigenvalues are real for real β_j, $j = 1, 2, 3$. The general solution of the conditionally linear system over T_i is written as

$$\bar{x}_j(t) = c_{2j-1} \exp(\beta_j(t - t_{i-1})) + c_{2j} \exp(-\beta_j(t - t_{i-1})), \quad j = 1, 2, 3, \tag{58}$$

where the arbitrary constants of integration are evaluated as

$$c_{2j-1} = x_{j,i-1}, \qquad c_{2j} = \dot{x}_{j,i-1} \quad \text{if } \beta_j = 0,$$

$$c_{2j-1} = 0{\cdot}5\left(x_{j,i-1} + \frac{\dot{x}_{j,i-1}}{\beta_j}\right), \qquad c_{2j} = 0{\cdot}5\left(x_{j,i-1} - \frac{\dot{x}_{j,i-1}}{\beta_j}\right) \quad \text{if } \beta_j \neq 0. \tag{59}$$

In the above equation, subscript j indexes the state variables while the other subscript i indexes the successive time instants. It may be noted that the uncoupled system of equations (57) could also have been so constructed as to have purely imaginary roots so that the solutions (58) are expressible in sine and cosine functions. However, from the solutions (58) it is evident that each uncoupled conditionally linear system in equation (57) has a uni-dimensional stable and unstable manifolds. One is therefore assured that locally unstable solutions (as for a chaotic orbit) in the original system are adequately simulated via the linearized system, presently adopted. The non-linear algebraic equations in terms of $\beta_j, j = 1, 2, 3$ may be formed, as usual, by substituting equation (58) in the original dynamical system (43) at $t = t_i$. For $\beta_j \neq 0, j = 1, 2, 3$, these transcendental equations are

$$\beta_1 c_1 \exp(\beta_1 h_i) - \beta_1 c_2 \exp(-\beta_1 h_i) - A[c_3 \exp(\beta_2 h_i) + c_4 \exp(-\beta_2 h_i) - c_1 \exp(\beta_1 h_i) - c_2 \exp(-\beta_1 h_i)] = 0, \tag{60a}$$

$$\beta_2 c_3 \exp(\beta_2 h_i) - \beta_2 c_4 \exp(-\beta_2 h_i) - (c_1 \exp(\beta_1 h_i) + c_2 \exp(-\beta_1 h_i))(R - c_5 \exp(\beta_3 h_i) - c_6 \exp(-\beta_3 h_i)) - B(c_3 \exp(\beta_2 h_i) + c_4 \exp(-\beta_2 h_i)) = 0, \tag{60b}$$

$$\beta_3 c_5 \exp(\beta_3 h_i) - \beta_3 c_6 \exp(-\beta_3 h_i) - (c_1 \exp(\beta_1 h_i) + c_2 \exp(-\beta_1 h_i))(c_3 \exp(\beta_2 h_i) + c_4 \exp(-\beta_2 h_i)) + B(c_5 \exp(\beta_3 h_i) + c_6 \exp(-\beta_3 h_i)) = 0. \tag{60c}$$

Similar developments regarding derivations of higher-level LTL systems for the HD oscillator, as in equation (37), are also possible. A possible (but not the only one) first-level LTL system for the HD oscillator may thus be conceived of as follows. Equation (37) is first differentiated with respect to t to yield

$$\dddot{x} + 2\pi\varepsilon_1 \ddot{x} + 4\pi^2 \varepsilon_2 (3x^2 + 1)\dot{x} = -8\pi^3 \varepsilon_3 \sin(2\pi t). \tag{61}$$

The form of equation (61) is suggestive of the following first-level LTL system:

$$\dddot{\bar{x}} + 2\pi\varepsilon_1 \ddot{\bar{x}} + 4\pi^2 \varepsilon_2 \beta \dot{\bar{x}} = -8\pi^3 \varepsilon_3 \sin(2\pi t), \tag{62}$$

where the conditional constant β, valid over the interval T_i, is related to $x(t_i) = x_i$ via the identity

$$\beta = 3x_i^2 + 1. \tag{63}$$

The conditionally linearized third order ODE, as given by equation (62) has got a one-dimensional central manifold corresponding to the zero eigenvalue. Over the interval T_i, the local initial conditions to equation (62) are $(x_{i-1}, \dot{x}_{i-1}, \ddot{x}_{i-1})$. It is essential to observe that $\ddot{x}_{i-1}$ should be expressed in terms of x_{i-1} and $\dot{x}_{i-1}$ using the given non-linear ODE (37). The rest of the derivations follow precisely the same steps as in the previous illustrations and are not repeated here.

7. NUMERICAL RESULTS

The numerical results presented here correspond to those obtained via the applications of zeroth- and first-level LTL methods, as explained in the previous section, to HD and Lorenz oscillators. In all the presentations to follow, the time-step size, h_i, for integration has been made constant for all i. To begin with, the DH oscillator is taken up. In the absence of any external forcing ad damping, i.e., $\varepsilon_3 = \varepsilon_2 = 0$, the oscillator is time-invariant Hamiltonian and has only one fixed point $(x, \dot{x}) = (0, 0)$ which is the centre. Thus, any non-zero initial condition corresponds to a distinct closed curve S^1, topologically equivalent to a circle. One such orbit, obtained via the zeroth-level LTL system, is shown in Figure 3 and compared with the orbit obtained using a sixth order Runge–Kutta scheme (RKGS). In case viscous damping is introduced without any external forcing ($\varepsilon_2 > 0, \varepsilon_3 = 0$), the erstwhile centre becomes a stable sink and the phase-space volume exponentially converge to zero. Evolution of one such trajectory, again obtained via zeroth

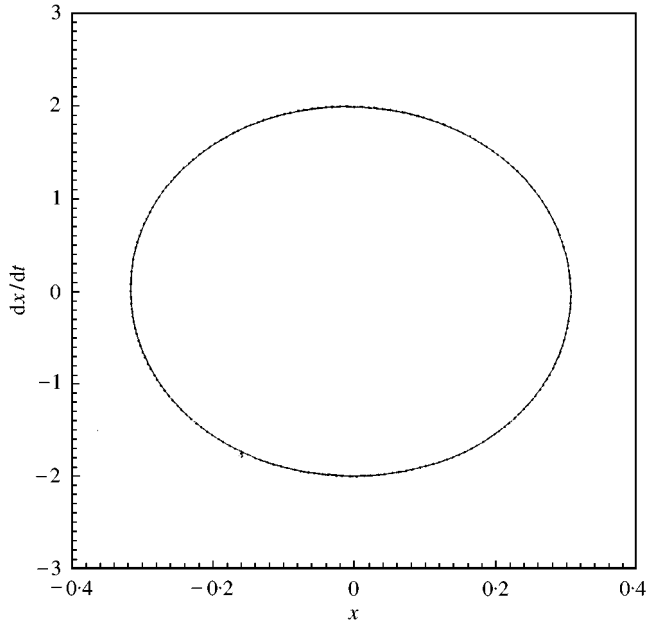

Figure 3. An unforced and undamped orbit of the HD oscillator, $\varepsilon_1 = 0{\cdot}0$, $\varepsilon_2 = 1{\cdot}0$, $\varepsilon_3 = 0{\cdot}0$, $h = 0{\cdot}01$: ——, RKGS; ·····, zeroth-level LTL.

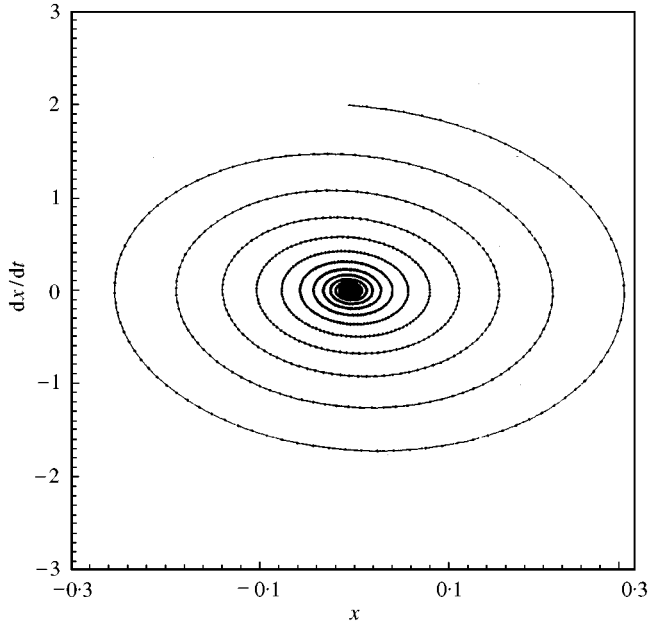

Figure 4. A viscously damped unforced orbit of the HD oscillator, $\varepsilon_1 = 0{\cdot}0$, $\varepsilon_2 = 1{\cdot}0$, $\varepsilon_3 = 0{\cdot}0$, $h = 0{\cdot}01$: ——, RKGS; ·····, zeroth-level LTL.

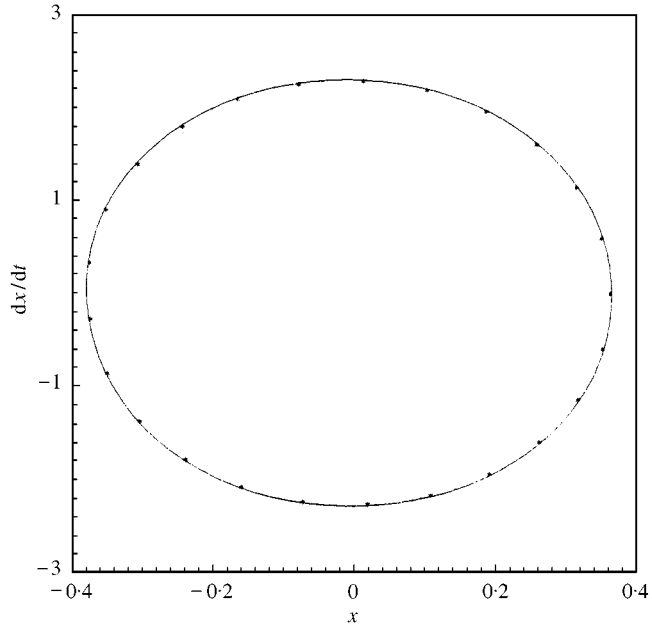

Figure 5. A forced elliptic 1-periodic orbit of the HD oscillator, $\varepsilon_1 = 0{\cdot}25$, $\varepsilon_2 = 1{\cdot}0$, $\varepsilon_3 = 0{\cdot}1$, $h = 0{\cdot}01$: ——, RKGS; ·····, zeroth-level LTL.

order LTL and RKGS schemes, is shown in Figure 4. If a 'small', non-zero, sinusoidal external forcing term is now added ($|\varepsilon_3| \ll 1$), the sink at (0, 0) undergoes a Hopf bifurcation to be an elliptic 1-periodic orbit, whose vibrating frequency is the same as that of the external force. Such an 1-periodic orbit, bearing strong resemblance of shape with the

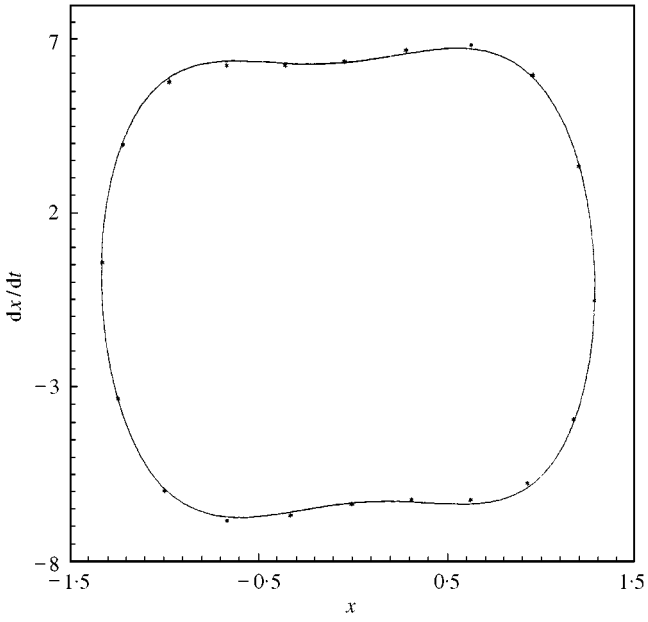

Figure 6. A dumb-bell shaped, almost symmetric 1-periodic orbit of the HD oscillator, $\varepsilon_1 = 0{\cdot}25$, $\varepsilon_2 = 1{\cdot}0$, $\varepsilon_3 = 1{\cdot}5$, $h = 0{\cdot}01$: ——, RKGS; ·····, zeroth-level LTL.

1-periodic orbit of a linear system under a sinusoidal excitation, is presently referred to as a small 1-periodic orbit. In Figure 5, one such small 1-periodic orbit is shown. It is interesting to note that while the trajectory (in time) of the orbit in Figure 3 is phase dependent, those corresponding to the orbits in Figures 4 and 5 are not. In all these cases, however, comparisons between the zeroth-level LTL and RKGS methods remain quite good. With increased values of the normalized forcing amplitude parameter, ε_3, the size of the 1-periodic orbit goes on increasing till it loses the elliptic shape to assume a dumb-bell-shaped structure, as shown in Figure 6. Further increases in ε_3 destroy the symmetry of these orbits and a couple of such unsymmetric periodic orbits are shown in Figures 7 and 8, both obtained using the zeroth-level LTL method. As seen from Figure 7(b), the orbit as plotted in Figure 7(a) is weakly phase dependent *with a very small time-varying phase angle* between two trajectories evolving with different initial conditions. The orbit of Figure 8, on the other hand, appears to be strictly phase independent (see Figure 8(b)). On an even more increases in ε_3, the orbit, as projected on the phase plane, crosses itself even while remaining periodic with the external frequency. Due to such self-intersections, the enclosed region in the phase plane no longer remains simply connected. A typical such phase plane projection, again produced by the zeroth-level LTL and compared, as usual, against a sixth order RKGS, is shown in Figure 9(a). As shown in Figure 9(b), the orbit is seen to be phase independent and hence the difference in the projected solutions on the phase plane via LTL and RKGS may be attributed to an error accumulation in the latter. Still higher values of ε_3 again produces self-intersecting periodic orbits in the phase plane, where the knotted areas enclosed by these intersections increase (Figure 10(a)). Incidentally, all these periodic orbits reported so far for $\varepsilon_3 > 0$ have been found to be phase independent. In Figure 10(b), for instance, time evolutions of two such trajectories, corresponding to the orbit in Figure 10(a) and starting with two different initial conditions, are reported. The phase independence is clearly observed and thus it is expected

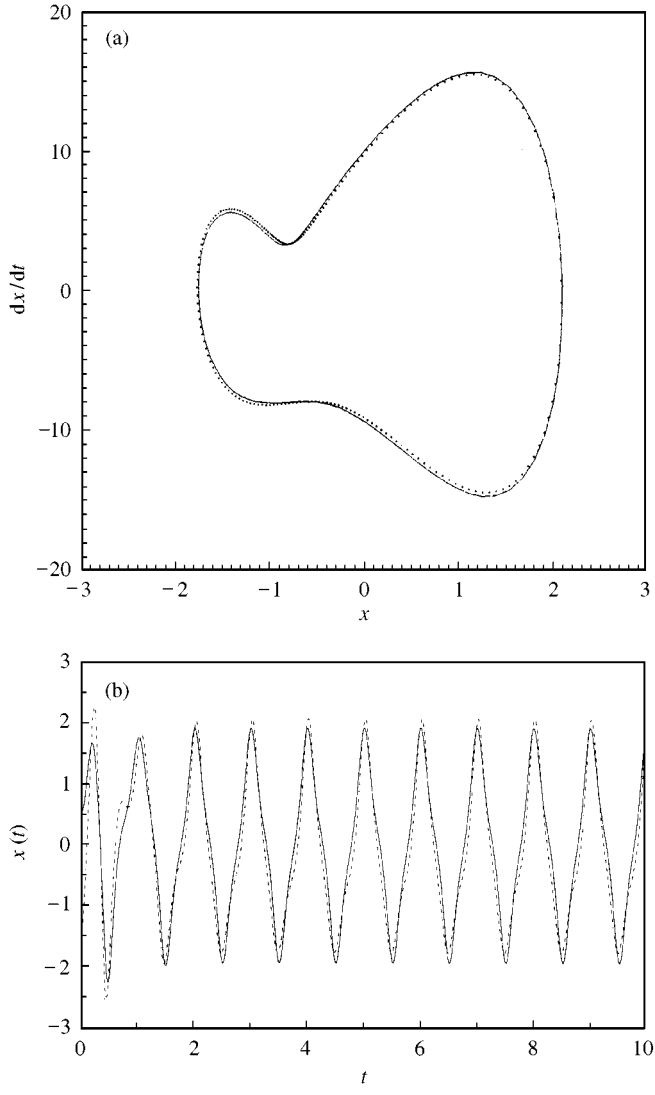

Figure 7. (a) An unsymmetric 1-periodic orbit of the HD oscillator, $\varepsilon_1 = 0{\cdot}25$, $\varepsilon_2 = 1{\cdot}0$, $\varepsilon_3 = 4{\cdot}0$, $h = 0{\cdot}005$: ——, RKGS; ·····, zeroth-level LTL. (b) Weak phase dependence of time histories.

that the zeroth-level LTL produces a more accurate orbit than RKGS. Chaotic orbits for the HD oscillator may be observed for very high values of the forcing amplitude parameter, ε_3. Since a chaotic orbit is very sensitively phase dependent, the zeroth-level LTL may be in error especially if the parameters are chosen near the stability boundaries of some other kind of solutions. One such strange attractor for the HD oscillator, obtained using RKGS, is shown in Figure 11. The parameter, ε_3, has been so chosen as to be close to the boundary where the periodic orbits of the type shown in Figure 10(a) loses stability. In this case, the zeroth-level LTL works to the extent of predicting a strange attractor, though of a little distorted shape, as shown in Figure 12(a) with $h = 0{\cdot}001$. With a still reduced step size of $h = 0{\cdot}0005$, the zeroth-level LTL yields the correct shape as reported in Figure 12(b). The first-level LTL, on the other hand, works quite well with $h = 0{\cdot}001$ and produces an attractor (shown in Figure 13) similar to the one in Figure 11.

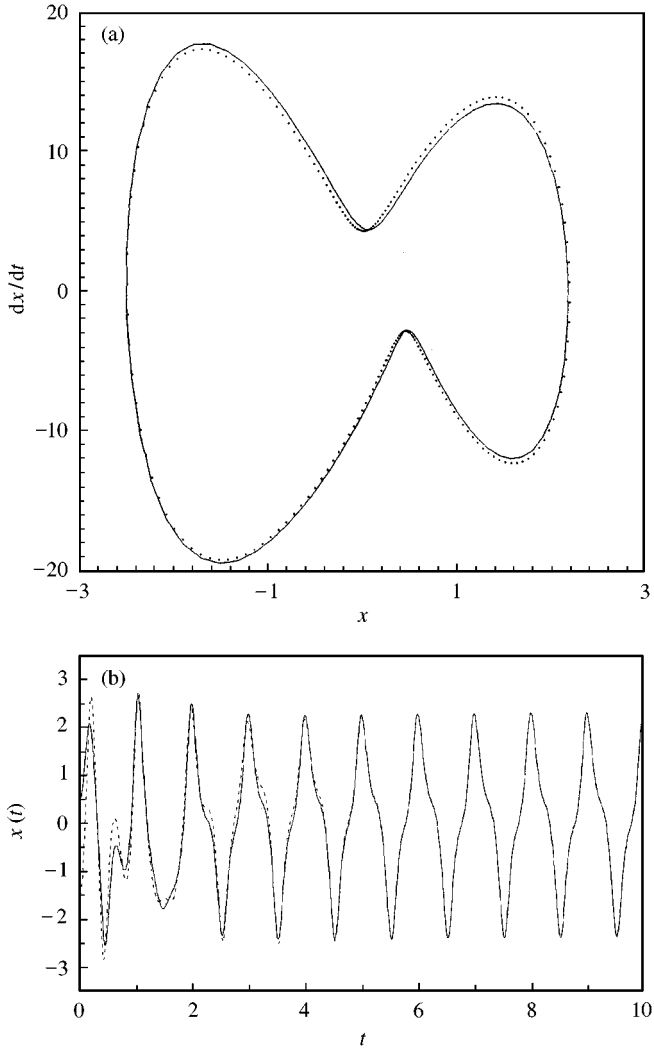

Figure 8. (a) An unsymmetric 1-periodic orbit of the HD oscillator, $\varepsilon_1 = 0{\cdot}25$, $\varepsilon_2 = 1{\cdot}0$, $\varepsilon_3 = 6{\cdot}0$, $h = 0{\cdot}005$: ——, RKGS; ·····, zeroth-level LTL. (b) Phase independence of time histories.

To describe the numerical results for the Lorenz system, the notations for the state variables x_1, x_2, x_3 will be conveniently replaced by x, y and z respectively. Unlike the HD system, the Lorenz oscillator is autonomous. A similarity with the HD oscillator, however, lies in that it is also dissipative having a negative divergence of $-(A + B + 1)$ for positive A and B. Here the point (0, 0, 0) remains a stable fixed point for $0 < r < 1$. A bifurcation occurs at $R = 1$ where the point (0, 0, 0) loses stability and two new stable fixed points are born. The co-ordinates of these fixed points are given by $(\sqrt{b(r-1)}, \sqrt{b(r-1)}, r-1)$ and $(-\sqrt{b(r-1)}, -\sqrt{b(r-1)}, r-1)$. Time histories of one such orbit approaching the fixed point with all positive coordinates is shown in Figure 14 along with a comparison with RKGS. It is seen that the path traced by the zeroth-level LTL almost always remains closer to the fixed point than the one traced by RKGS. It is clear that while applying the zeroth-level LTL procedure to such phase-independent solutions, relatively higher

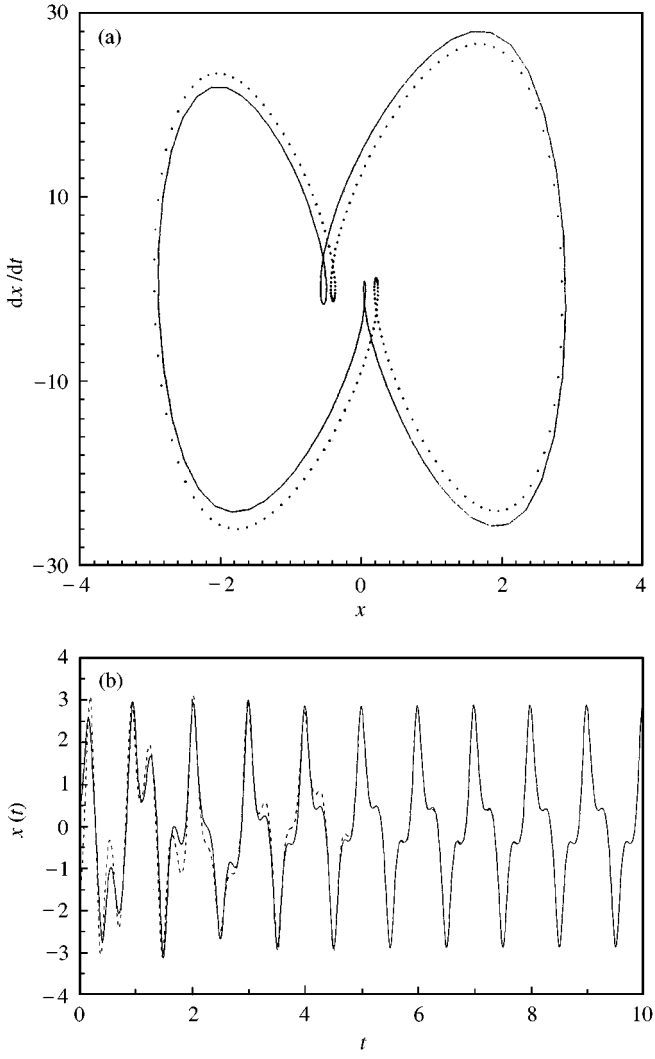

Figure 9. (a) An unsymmetric, self-intersecting periodic orbit of the HD oscillator, $\varepsilon_1 = 0{\cdot}1$, $\varepsilon_2 = 1{\cdot}0$, $\varepsilon_3 = 9{\cdot}0$, $h = 0{\cdot}005$: ——, RKGS; ·····, zeroth-level LTL. (b) Phase independence of time histories.

time-step sizes may be chosen. In the present case, the time step has been uniformly chosen to be 0·1. It is known that in the range $24{\cdot}06 < R < 24{\cdot}74$, in addition to the two stable fixed points as mentioned above, a strange attractor also co-exists. In Figure 15(a), a typical trajectory, attracted by one of these two fixed points and produced using the zeroth-level LTL, is shown for $R = 24{\cdot}10$. It may be seen that the value of R has been chosen close to the left boundary of the interval $24{\cdot}06 < R < 24{\cdot}74$. It has once again been observe that only a distorted strange attractor is obtainable with the use of zeroth-level LTL (equation (44) only) for this value of R. The first-level LTL, however, remains relatively accurate, as is shown in Figure 15(b). For $R > 24{\cdot}74$, the two fixed points lose their stability and only the strange attractor exists. As a final check on the zeroth-level LTL as applied to phase-independent solutions, a trajectory corresponding to $R = 24{\cdot}73$ is shown in Figure 16. The initial condition for this trajectory has been so chosen that it is attracted by the fixed

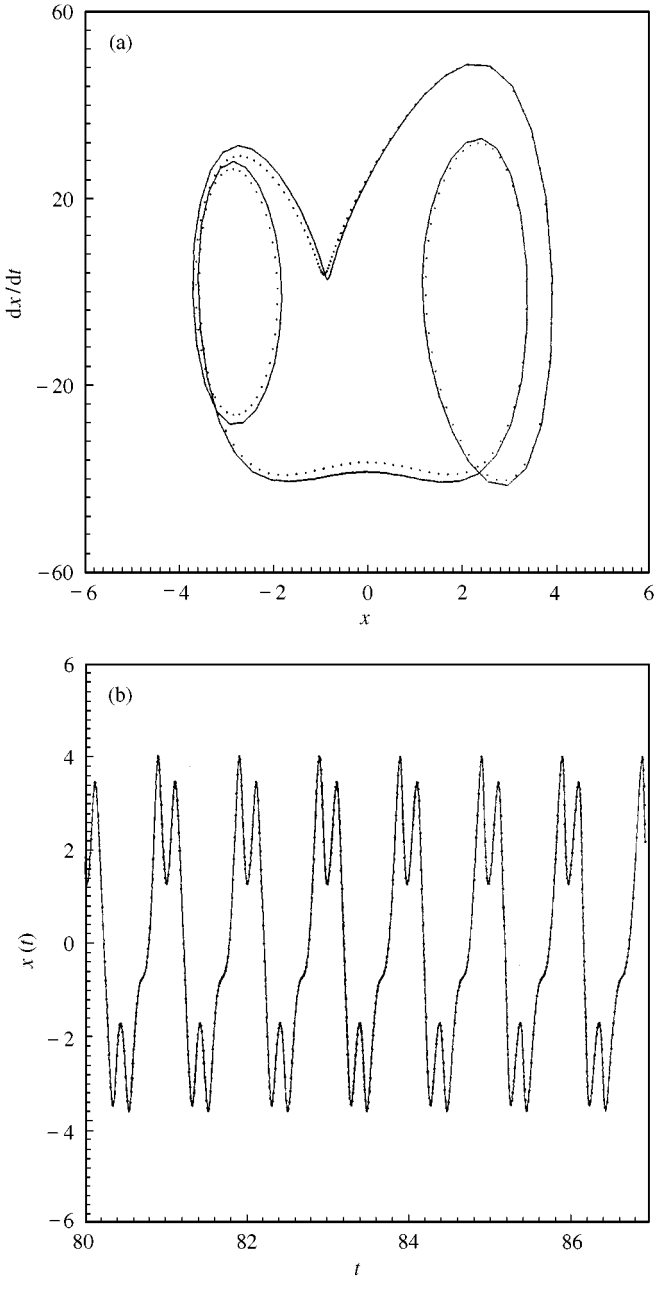

Figure 10. (a) A typical unsymmetric, self-intersecting periodic orbit of the HD oscillator preceding chaos, $\varepsilon_1 = 0{\cdot}25, \varepsilon_2 = 1{\cdot}0, \varepsilon_3 = 25{\cdot}0, h = 0{\cdot}005$: ——, RKGS; ·····, zeroth-level LTL; (b). Phase independence of the orbit of Figure 10(a): ——, $x\ (0) = 0$, $\mathrm{d}x(0)/\mathrm{d}t = 0$; ····· $x(0) = 0$, $\mathrm{d}x(0)/\mathrm{d}t = 1{\cdot}0$.

point with all positive co-ordinates. It has been observed that starting from $t = 0$, the trajectory goes within a neighbourhood with a radius of the order of 10^{-08} at the end of $t = 20$. In fact, for choices of parameters sufficiently away from the stability boundaries of other solutions, the zeroth-level LTL (equation (44) only) produces the strange attractors fairly accurately. One such strange attractor for $R = 40$ is shown in Figure 17.

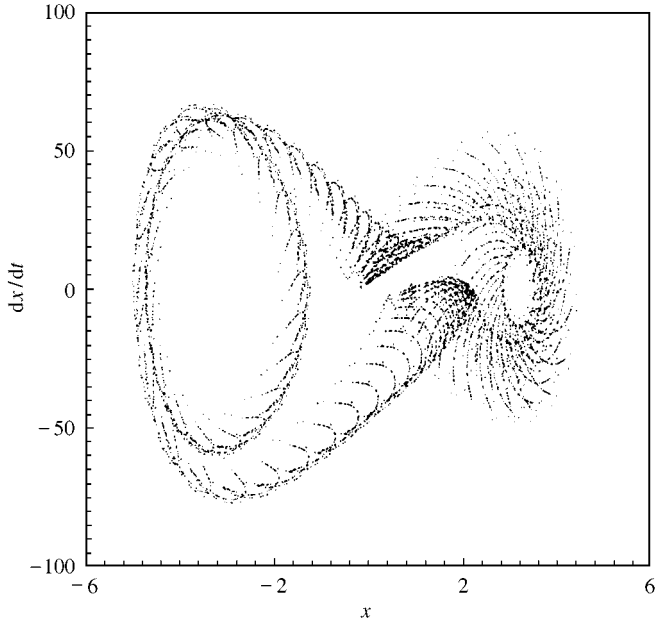

Figure 11. A strange attractor of the HD oscillator via RKGS, $\varepsilon_1 = 0{\cdot}25$, $\varepsilon_2 = 1{\cdot}0$, $\varepsilon_3 = 41{\cdot}0$, $h = 0{\cdot}001$.

8. DISCUSSION AND CONCLUSIONS

A new local linearization procedure, called the locally transversal linearization (LTL), for analyses and simulations of non-linear ODEs (posed as initial value problems) is outlined in this study. Put in a nutshell, given a non-linear dynamical system and relevant initial conditions, the LTL method strives to find out a set of conditionally linear dynamical systems, each having its validity over a chosen time interval. To be precise, given a time interval and the known state vector (initial condition) at the beginning of the interval, the corresponding conditionally linear system may be constructed in such a way as to transversally intersect the non-linear trajectory at the end of the interval. The conditional linearity of these derived dynamical systems stems from the fact that the desired solution vector itself enters the equations as parameters. The postulated condition of transversal intersection between the original and linearized trajectories at the right end of the chosen time interval leads to a system of non-linear algebraic (transcendental) equations in terms of these unknown parameters or the solution vector. Thus, the LTL procedure essentially attempts to break up a given non-linear dynamical system into a correct Poincare map over the given time step. While this map is exact modulo the floating-point error in the phase-dependent regime, errors do creep in if the solution is sought in the phase-dependent regime. A theoretical error analysis based on Bellman–Grownwall lemma suggests an error upper bound of the order of the chosen time step during the transient regime. Such a bound points to the possibility of undesirable inaccuracies in the phase-independent cases, especially for cases where the parameters are chosen close to the stability boundaries. One way to avoid such inaccuracies is to construct higher-level LTL systems, where additional initial conditions in terms of the derivatives of the original vector field are incorporated for constructing the locally linearized orbit. In this way, it becomes possible to introduce a path sensitivity in the LTL system. In the present study, limited results presented only for a few

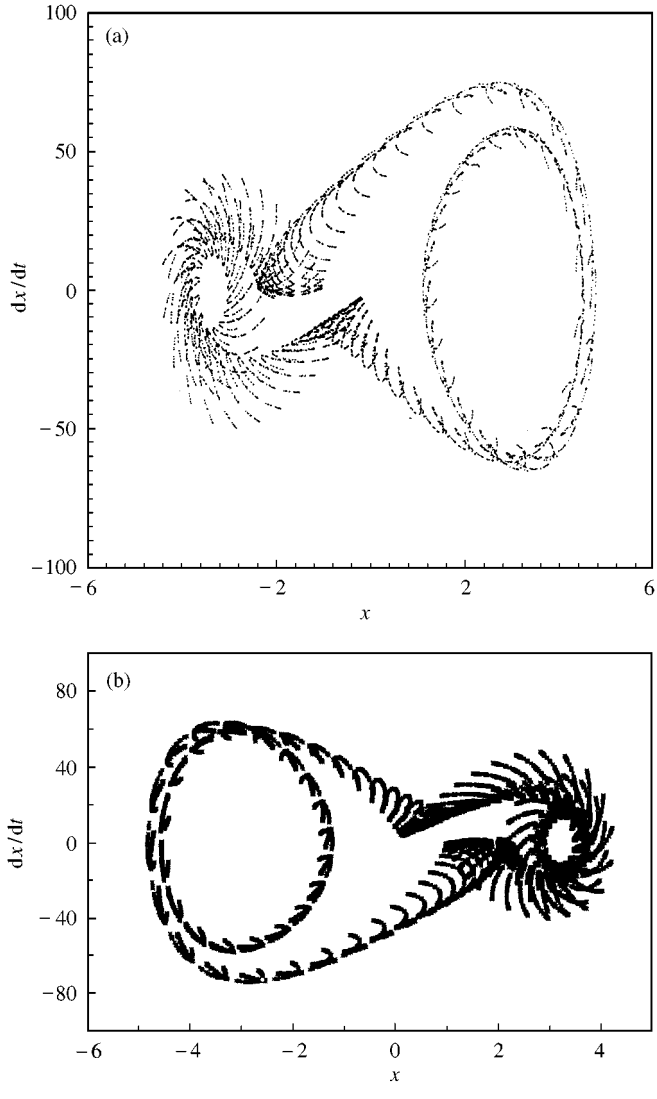

Figure 12. (a) An inaccurate shape of the strange attractor of Figure 11 via zeroth-level LTL, $h = 0{\cdot}001$; (b) an accurate shape of the strange attractor with $h = 0{\cdot}0005$.

first-level LTL systems indeed point to an improved numerical accuracy. The procedure to construct zeroth- and higher-level LTL systems is non-unique and this particular feature may be well exploited to construct conditionally uncoupled LTL systems with very simple forms. It is worth noting here that the procedures outlined in this paper to derive the LTL systems for the Lorenz oscillator may be adapted to a general m.d.o.f. non-linear dynamical system with hardly any further modifications.

The conditional linearization achieved via the principles of LTL may be construed either as a flow or a map. Either way, the analytical nature of the flow or the diffeomorphism may be exploited to achieve a lot more than is done presently. For example, the basic concept of LTL may as well be made applicable to a large class of non-linear boundary value problems, governed by non-linear ODEs and of immense use in static and dynamic

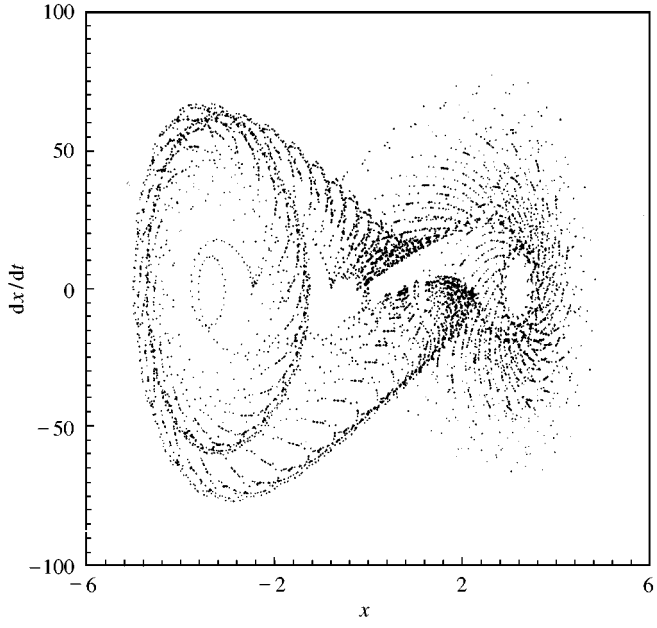

Figure 13. The strange attractor of Figure 11 via first-level LTL.

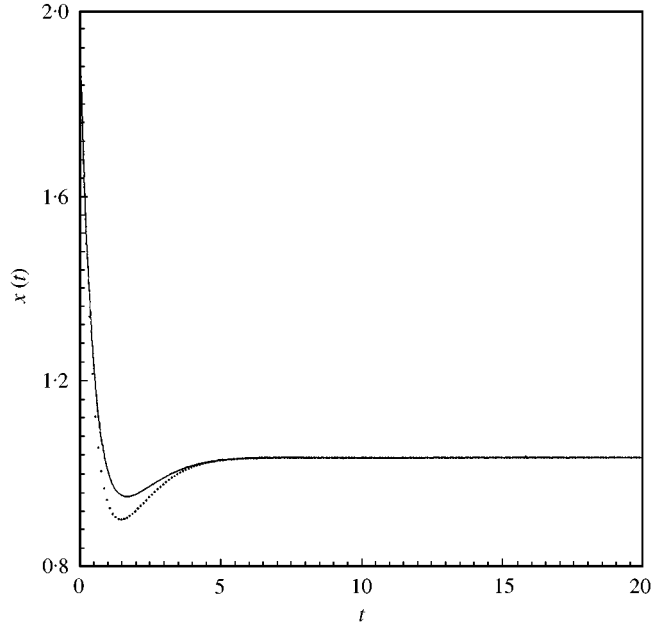

Figure 14. A trajectory approaching a stable fixed point of the Lorenz system, $A = 10$, $B = 8/3$, $R = 1{\cdot}4$, $h = 0{\cdot}1$: ——, zeroth-level LTL; ·····, RKGS.

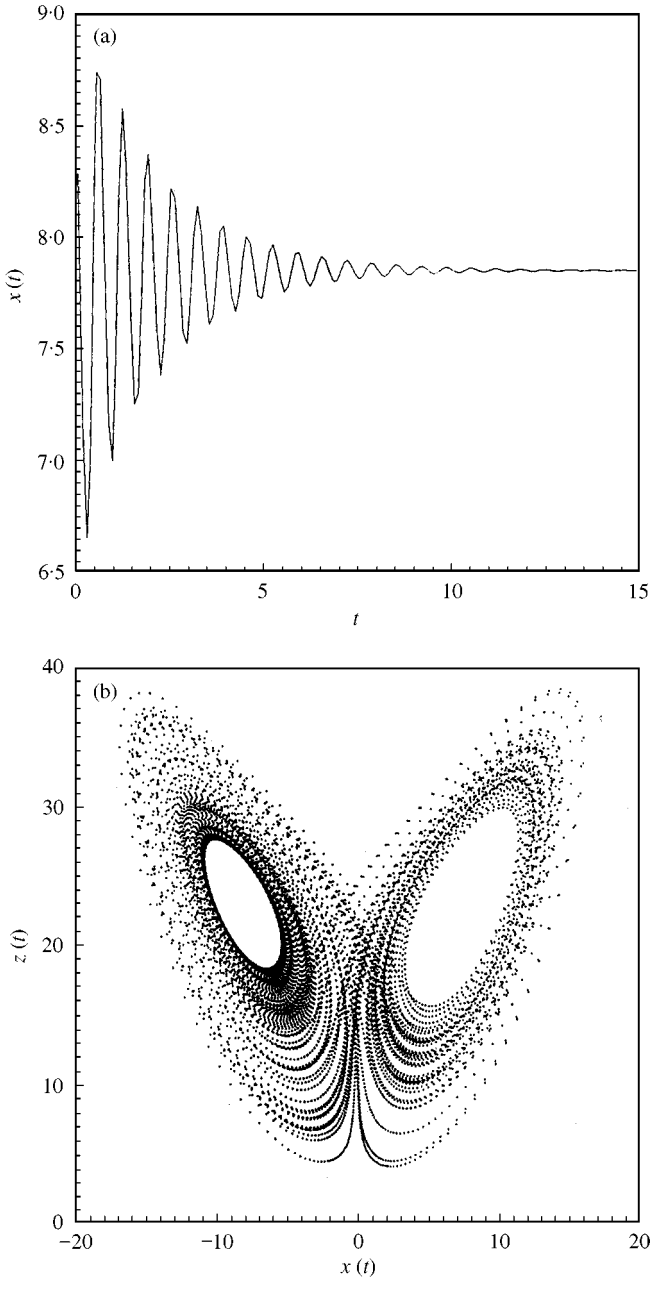

Figure 15 (a) A trajectory approaching a stable fixed point of the Lorenz system, $A = 10$, $B = 8/3$, $R = 24{\cdot}1$, $h = 0{\cdot}1$; (b) A strange attractor of the Lorenz system via first-level LTL (parameters as in Figure 15(a), except that $h = 0{\cdot}001$).

problems of structural mechanics. Moreover, the same principles may be extended a little to treat stochastic ODEs. This may shed some light on questions regarding optimizations of certain reliability measures. Questions regarding the extensions of LTL principles for dynamical systems with various kinds of discontinuities in the vector fields also remain more or less unresolved at this stage.

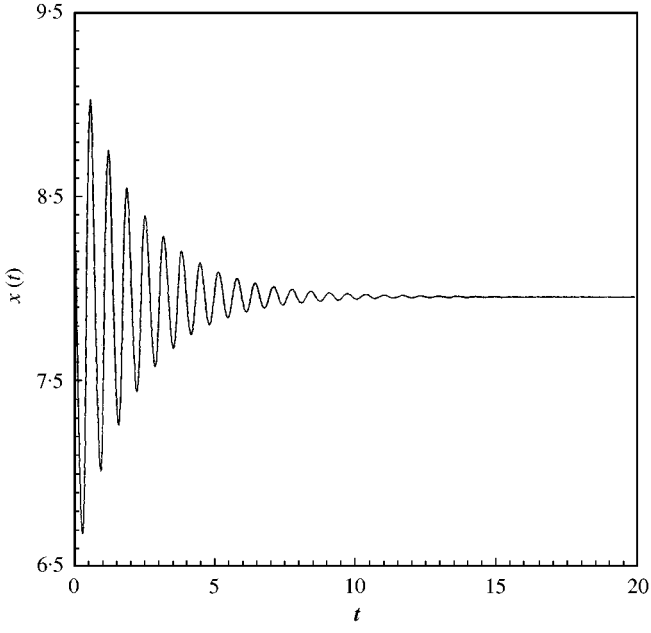

Figure 16. A trajectory approaching a stable fixed point of the Lorenz system, $A = 10$, $B = 8/3$, $R = 24{\cdot}73$, $h = 0{\cdot}1$.

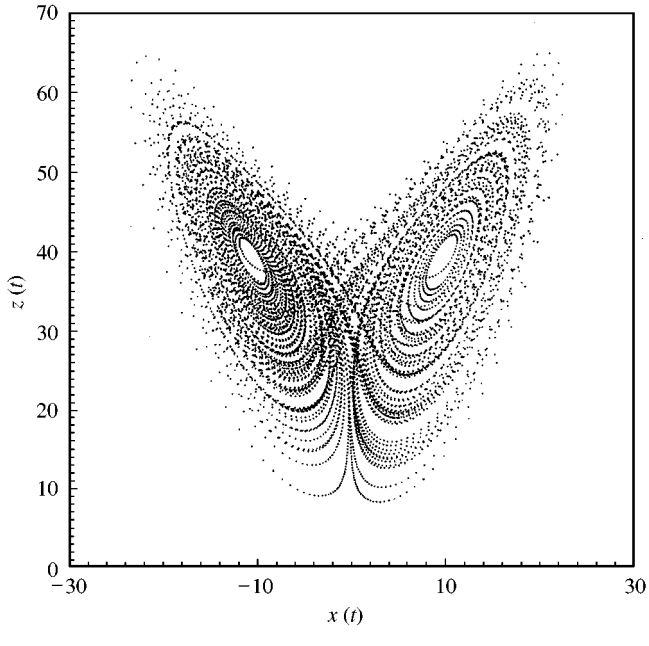

Figure 17. A typical strange attractor of the Lorenz system via zeroth-level LTL, $A = 10$, $B = 8/3$, $R = 40{\cdot}0$, $h = 0{\cdot}001$.

REFERENCES

1. Y. A. MITROPOLSKI 1965 *Problems of the Asymptotic Theory of Non-stationary Vibrations*. New York: Daniel Davey.
2. A. H. NAYFEH 1981. *Introduction to Perturbation Techniques*. New York: John Wiley & Sons.
3. A. J. LICHTENBERG and M. A. LIEBERMAN 1982 *Regular and Stochastic Motion*. Berlin: Springer-Verlag.
4. A. H. NAYFEH and D. T. MOOK 1979 *Nonlinear Oscillations*. New York: John Wiley & Sons.
5. A. H. NAYFEH 1984 *Journal of Sound and Vibration* **88**, 1–10. Combination tones of single-degree-of-freedom systems with quadratic and cubic non-linearities.
6. S. L. LAU and Y. K. CHEUNG 1981 *Journal of Applied Mechanics* **48**, 959–964. Amplitude incremental variational principle for nonlinear vibration of elastic systems.
7. J. M. ORTEGA and W. C. RHEINBOLDT 1970 *Iterative solutions of Non-linear Equations in Several Variables*. New York: Academic Press.
8. S. J. LIAO 1992 *Journal of Applied Mechanics* **59**, 970–975. A second order approximate analytical solution of a simple pendulum by the process analysis method.
9. M. YAMAGUTI and S. USHIKI 1981 *Physica D* **3**, 618–626. Chaos in numerical analysis of ordinary differential equations.
10. E. N. LORENZ 1989 *Physica D* **35**, 299–317. Computational chaos: a prelude to computational instability.
11. R. N. IYENGAR and D. ROY 1998 *Journal of Sound and Vibration* **211**, 843–875. New approaches for the study of non-linear oscillators.
12. R. N. IYENGAR and D. ROY 1998 *Journal of Sound and Vibration* **211**, 877–906. Extensions of the phase space linearization (PSL) technique for non-linear oscillators.
13. D. ROY 2000 *Journal of Sound and Vibration* **231**, 307–341. Phase space linearization for non-linear oscillators: deterministic and stochastic system.
14. R. N. IYENGAR and D. ROY 1999 *Proceedings of the IUTAM Symposium On Nonlinearity and Stochastic Structural Dynamics*. Dordrecht: Kluwer Academic Publishers. Application of conditional linearization in the study of non-linear systems.
15. D. R. J. CHILLINGWORTH 1976 *Differential Topology with a View to Applications*. London: Pitman.
16. P. HARTMAN 1964 *Ordinary Differential Equations*. New York: Wiley.
17. V. I. ARNOLD 1983 *Geometrical Methods in the Theory of Ordinary differential Equations*. Berlin: Springer-Verlag.
18. J. HALE 1980. *Ordinary Differential Equations*. Malabar, FL: Robert E. Krieger Publishing Co., Inc.
19. YU, YI-YUAN 1995 *Vibration of Elastic Plates*. Berlin: Springer-Verlag.
20. D. A. RAND 1978 *Mathematical Proceedings of the Cambridge Philosophical Society* **83**, 451–460. The topological classification of Lorenz attractors.
21. C. SPARROW 1982 *The Lorenz Equations*: *Bifurcation*, *Chaos and Strange Attractors*. Berlin: Springer.
22. L. RADE and B. WESTERGREN 1990 *BETA Mathematics Handbook*. Chartwel-Bratt; Second edition, Lund, Sweden.